An Integrated Landslide Susceptibility Mapping of Wayanad district, Kerala using AHP and FR Models: A Lessons from the 2024 Landslides

Akhil Tej S.[1]*, Ramya Swetha R.[2], Venkata Rami Reddy Y.[3], Padma Priya K.T.[4] and Vishnu Vardhan Reddy L.[5]

1. Department of Civil Engineering, G. Pullaiah College of Engineering and Technology, Kurnool, Andhra Pradesh, INDIA
2. Department of Civil Engineering, Institute of Aeronautical Engineering, Dundigal, Hyderabad, Telangana, INDIA
3. Department of Civil Engineering, SVR Engineering College, Nandyal, Andhra Pradesh, INDIA
4. Department of H&S, CVR College of Engineering, Ibrahimpatnam, Hyderabad, Telangana, INDIA
5. Department of Civil Engineering, University College of Engineering JNTUK, Narasaraopet, INDIA

*akhiltej147@gmail.com

Abstract

This study presents a comprehensive landslide susceptibility mapping (LSM) for Wayanad district using a Multi-Criteria Decision-Making (MCDM) approach, integrating Geographic Information Systems (GIS) with the Analytical Hierarchy Process (AHP) and Frequency Ratio (FR) models. The methodology involves a six-step process: data collection from USGS, SRTM-DEM and Bhukosh followed by the creation of thematic maps covering elevation, slope, aspect, proximity to roads and rivers, geological features, rainfall and land use/land cover. AHP is applied by rescaling thematic maps to a uniform 5-point scale, calculating the consistency index and determining weights. If the consistency ratio (CR) is ≥ 0.10, adjustments are made to ensure accuracy. FR values for each factor are computed to develop the LSM.

The LSM was validated using Receiver Operating Characteristic (ROC) curves and Area under the Curve (AUC) values, with AUC scores of 0.913 and 0.896 for the AHP and FR models, respectively indicating high prediction accuracy. The LSM is categorized into five susceptibility classes: very low, low, moderate, high and very high, providing critical insights for disaster preparedness and risk mitigation in Wayanad. The study underscores the significant role of GIS and MCDM techniques in enhancing landslide risk assessment and management.

Keywords: Landslides, Wayanad, Geographical Information System, Analytical Hierarchy Process, Weighted Overly Technique.

Introduction

Wayanad, a district in the Western Ghats of Kerala, India, is renowned for its scenic landscapes, unique biodiversity and agricultural economy. However, this region also faces recurring threats from landslides, especially during the intense monsoon season[8]. The Western Ghats, listed as one of the eight hottest hotspots of biodiversity in the world, are highly susceptible to various natural hazards due to their rugged terrain, steep slopes, heavy seasonal rainfall and increasing anthropogenic activities[1]. In recent years, landslide occurrences have escalated, driven by deforestation, unregulated construction and agricultural expansion on the hilly terrains, making the region's communities and economy vulnerable to these disasters[3].

The 2024 landslides in Wayanad highlighted the critical need for effective landslide susceptibility mapping and risk mitigation strategies. These landslides, triggered by unprecedented rainfall and other contributing factors, not only led to significant loss of life and property but also disrupted local infrastructure and economic activities, especially impacting the agricultural sector[11]. Additionally, these landslides increased awareness of the long-term environmental impact on the region's ecological balance. As a result, there is an urgent demand for more comprehensive landslide susceptibility studies to identify risk areas, which can help to inform disaster preparedness, to guide safe land use practices and shape sustainable development policies[7].

Understanding landslide susceptibility is essential in regions like Wayanad where multiple factors (e.g. rainfall intensity, soil composition, slope gradient and human activities) interplay in complex ways[2]. Landslide susceptibility mapping enables the identification of areas with varying degrees of landslide risk which is essential for establishing early warning systems, planning evacuation routes and designating safe zones for construction[25]. By developing an accurate, data-driven susceptibility model, stakeholders, including government agencies, environmental planners and local communities, can make informed decisions that prioritize safety and sustainability in Wayanad.

Relevance and Significance of GIS and AHP in Susceptibility Mapping: Geographic Information Systems (GIS) and the Analytical Hierarchy Process (AHP) are essential tools for landslide susceptibility mapping, especially in geologically diverse and ecologically sensitive regions like Wayanad. GIS allows for the integration, visualization and spatial analysis of multiple datasets across varied domains including topography, geology, climate and land use. In landslide studies, GIS is particularly useful for developing thematic maps that represent factors influencing landslide susceptibility such as slope gradient, soil type and rainfall distribution. By using GIS, researchers can create a multi-layered map that combines these thematic layers into a composite landslide susceptibility map, revealing high, moderate and low-risk zones across the region.

The AHP is a multi-criteria decision-making (MCDM) tool that assigns weights to each factor influencing landslide susceptibility based on its relative importance[47]. Developed by Saaty, AHP is widely recognized for its structured, mathematical approach to decision-making, which is particularly valuable in complex environmental studies. In the context of landslide susceptibility mapping, AHP enables the quantification of the significance of each factor (e.g. slope, soil type, vegetation cover) based on expert judgment or empirical data, thus providing a scientifically grounded way to weigh each factor's impact on landslide risk[4-6].

Integrating GIS with AHP provides a robust framework for landslide susceptibility mapping. GIS effectively handles spatial data while AHP facilitates the analytical rigor needed to prioritize the various factors based on their contribution to landslide risk[9]. This integration helps to generate a susceptibility model that reflects both the physical characteristics of the terrain and the insights of subject-matter experts, ensuring a comprehensive approach. Such a model can be validated with historical landslide data, increasing its predictive accuracy and making it a valuable resource for proactive risk management.

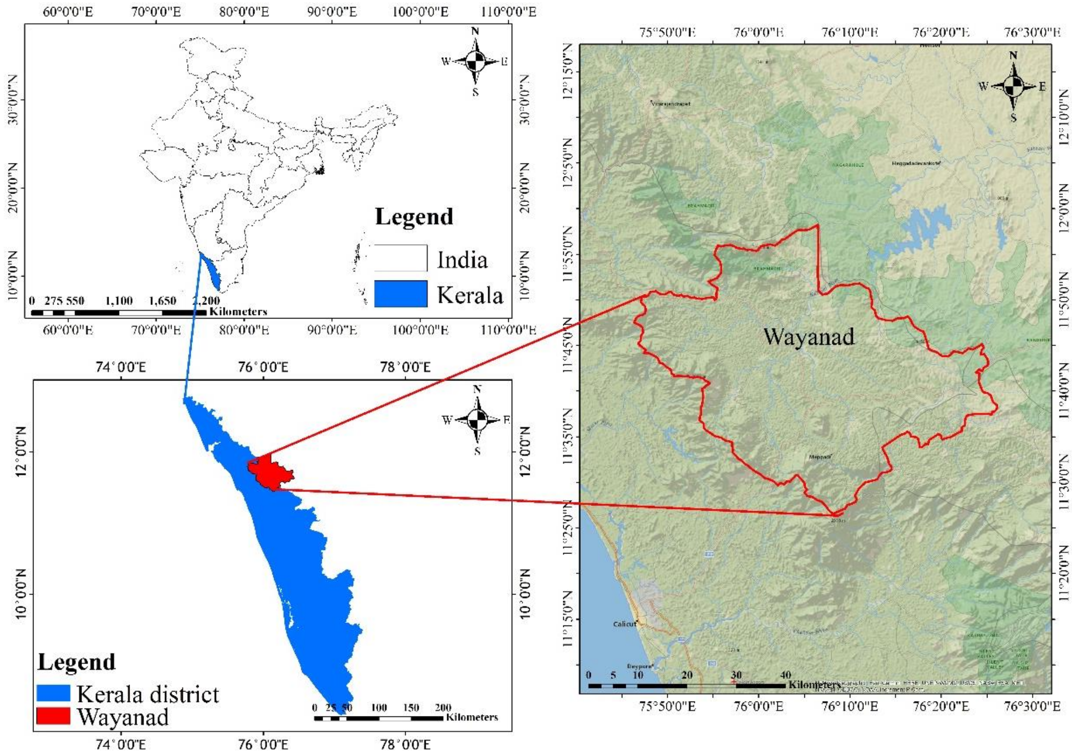

Fig. 1: Geographical location map of the Wayanad district from Kerala.

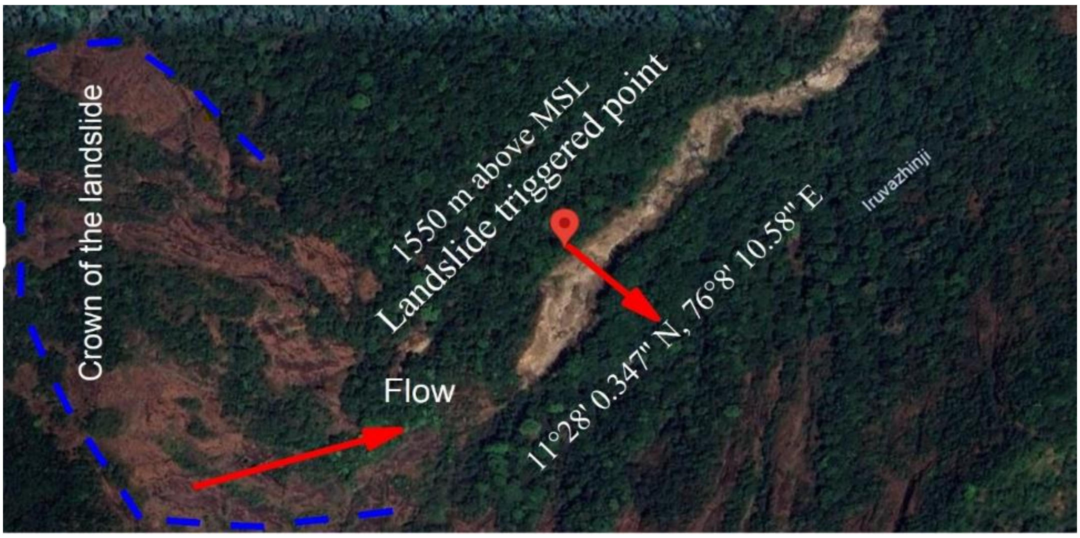

Fig. 2: Details of the 30th of July 2024 Wayanad landslide and flow pattern

In the context of Wayanad, applying GIS and AHP to landslide susceptibility mapping offers several benefits[38]. First, it enables the identification of risk-prone areas, aiding in the planning of safe zones for infrastructure and settlement development. Secondly, it supports local authorities in developing targeted mitigation strategies, such as reinforcing vulnerable slopes or restricting land use in high-risk zones. Lastly, the resulting map can be used to educate local communities about landslide risks, contributing to greater awareness and preparedness[10].

Surface feature with initial values and Geographic and climatic characteristics: Wayanad is a picturesque hill district located in the northeastern part of Kerala, bordered by the Western Ghats. The geographical location map of the Wayanad state boundary is shown in figure 1. The Wayanad spans an area of approximately 2,131 km², featuring undulating terrain, lush green valleys and a predominantly rural landscape[9]. The district, established in its current form on November 1, 1980, was created by merging North Wayanad and South Wayanad, which were previously part of Cannannore (now Kannur) and Kozhikode districts respectively[11]. Presently, Wayanad is organized into three tehsils: Vythiri, Mananthavady and Sulthan Bathery and four administrative blocks: Kalpetta, Mananthavady, Panamaram and Sulthan Bathery, with Kalpetta as the sole municipality.

The structure provides a framework for governance and local administration across its 25-gram panchayats. Geographically, Wayanad is characterized by its hilly terrain and high-altitude plateaus with elevations ranging from 700 to 2,100 meters above sea level. The spatial distribution of elevation with 30-meter resolution and slope map of the Wayanad is shown in figure 3.

The primary objectives of this study are to analyze the landslide susceptibility mapping of Wayanad through a MCDM approach, integrating Geographic Information Systems (GIS) with the AHP and Frequency Ration (FR) models. By focusing on Wayanad's geographic, climatic and socio-economic characteristics, the study aims to provide a comprehensive landslide susceptibility map that can serve as a tool for risk mitigation and disaster preparedness[23]. Additionally, the study seeks to examine how recent landslides, particularly those in 2024, influence susceptibility patterns, emphasizing the importance of sustainable land use and community awareness in reducing landslide impacts[24]. This research will contribute to a deeper understanding of the spatial distribution of landslide risks and will help in future disaster management and planning initiatives to build resilience against landslides in Wayanad[18].

Material and Methods

The methodology for landslide susceptibility mapping involves a multi-step process. Initially, data from USGS, SRTM-DEM and Bhukosh sources are collected (Step I). Data is further utilized to create thematic maps including parameters such as elevation, slope, aspect, proximity to roads and rivers, geological and geomorphological features, rainfall and land use/land cover (Step II). In Step III, the AHP is implemented by rescaling all thematic maps to a uniform 5-point scale, followed by the calculation of the consistency index and frequency ratio. The weights of indicators are determined and validated for consistency (Step IV).

If the consistency ratio (CR) is ≥ 0.10, adjustments are made before weight calculation. Subsequently, indices are calculated (Step V), leading to the generation of the landslide susceptibility map. The performance of the assessment is evaluated to ensure accuracy and reliability (Step VI)[13-15]. The detailed step by step methodology is shown in figure 4.

Wayanad experiences a tropical monsoon climate with distinct wet and dry seasons. The district receives an average annual rainfall of about 3,000 mm, mainly concentrated during the southwest monsoon season from June to September, with an additional contribution from the northeast monsoon between October and December. The heavy monsoon rains, combined with Wayanad's steep slopes and varied soil types, contribute to its susceptibility to landslides, especially in regions with high deforestation or agricultural activity[17].

During the dry season which spans from December to March, the region experiences milder weather, with temperatures ranging between 15°C and 29°C, although higher altitudes often experience cooler conditions[16]. The district's distinct geography and climatic conditions, combined with a predominantly agricultural economy and large tribal population, make it unique within Kerala. However, these same factors also contribute to its vulnerability to natural hazards like landslides, especially in the wake of climate change and increased monsoonal variability[18]. The 2024 landslides underscored the urgent need for landslide susceptibility mapping and effective risk mitigation strategies, as they caused widespread disruption to live, property and agriculture[34].

The details of crown, flow path and elevation point of 30th July 2024 landslide is shown in figure 2 and the associated damage is shown in figure 5. Understanding Wayanad's geographic and climatic profile is thus essential for developing sustainable disaster preparedness and land management policies, ensuring both environmental preservation and the resilience of local communities[41-43].

History of landslides and its impact on Wayanad: Wayanad's landslide history reflects a long-standing vulnerability stemming from its geographic and climatic context in the Western Ghats. Documentation of landslide events began in earnest in the late 20th century, with a surge in recorded incidents in recent decades as both rainfall intensity and land-use changes increased.

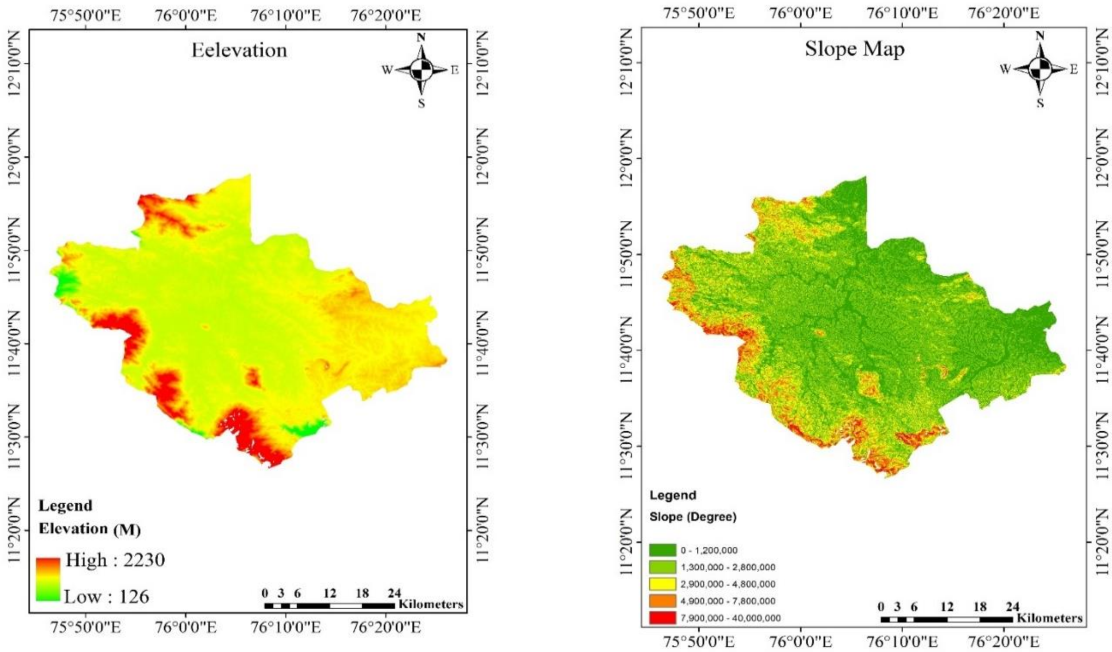

Fig. 3: The elevation with 30 m resolution and slope map of the Wayanad district

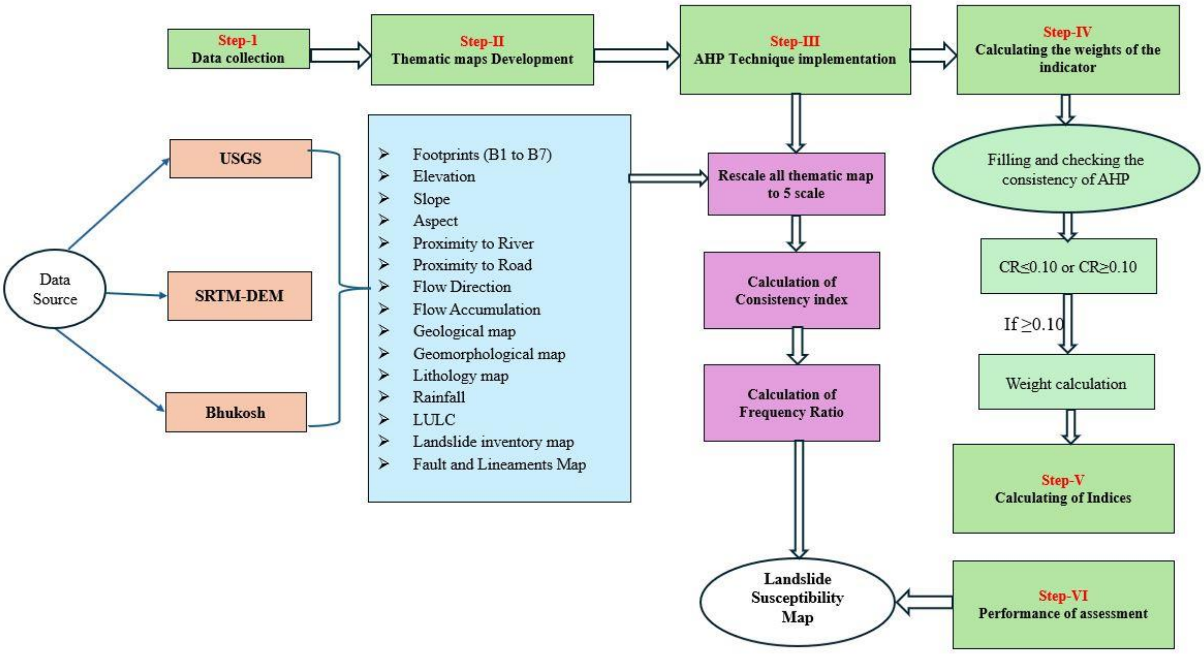

Fig. 4: Flow chart shows the methodology used in the present study for landslide susceptibility mapping of the Wayanad district.

Fig. 5: Few effected areas during the 30th of July 2024 landslide showing the soil erosion and floods (Source: online)

Notably, in 2018 and 2019, Wayanad witnessed catastrophic landslides following unprecedented monsoon rains, which caused severe flooding and landslides throughout Kerala. The 2018 landslides were triggered by record-breaking rainfall that saturated the soils and destabilized the terrain across the district[19]. In 2019, another massive landslide event occurred in the Puthumala and Meppadi areas, leading to widespread destruction of homes, agricultural land and infrastructure.

The event highlighted the compounded vulnerability of Wayanad's communities, many of which reside in high-altitude areas prone to landslides due to deforestation and unregulated development. The recent 2024 landslides further underscored this susceptibility, as intense monsoonal activity resulted in soil saturation and slope failures, causing significant disruptions. Each major landslide event emphasizes the growing landslide risk due to combination of natural and anthropogenic factors, underscoring the urgent need for systematic landslide susceptibility mapping and disaster preparedness in the region[20-22].

Results and Discussion

The characteristics of surface features including geology, geomorphology, lithology and LULC mapping are detailed here. Flow characteristics, such as flow direction and accumulation, are also crucial factors influencing landslides and are spatially represented. The AHP and FR techniques were employed to calculate weights based on priority. By integrating all thematic maps using GIS, the landslide susceptibility map for the Wayanad district was successfully developed[25].

Geological features of Wayanad: Wayanad district's geology is categorized into four main geological domains: the Peninsular Gneissic complex in the northern and central regions, the Migmatite complex in the south-central region, the Charnockite Group in the south and the Wayanad group in the north. The Wayanad group, consisting of supracrustal rocks, includes garnet-sillimanite-biotite gneiss (with or without graphite), kyanite-fuchsite-muscovite-quartz schist, hornblende-biotite schist, amphibolite bands, quartz-sericite schist and meta-ultramafic rocks[26]. These represent metamorphic facies from upper amphibolite to lower granulite, found mainly as linear bands in the northern region. The key member, garnet-sillimanite-biotite gneiss with graphite, occurs prominently north of the Kabani River. The Peninsular Gneissic complex, represented by hornblende-biotite and pink granite gneiss, covers a large portion of the district. The Charnockite group, forming the hilly southern terrain, consists of pyroxene granulite and banded magnetite quartzite interspersed within charnockite[26].

The Migmatite complex, primarily biotite-hornblende gneiss occupies extensive areas in the south-central part, with garnetiferous quartz-feldspathic gneiss and sillimanite occurring as narrow bands within older charnockite formations. Intrusive formations of pink granite are found near Kalpetta and Sultan Bathery, along with associated pegmatite veins.

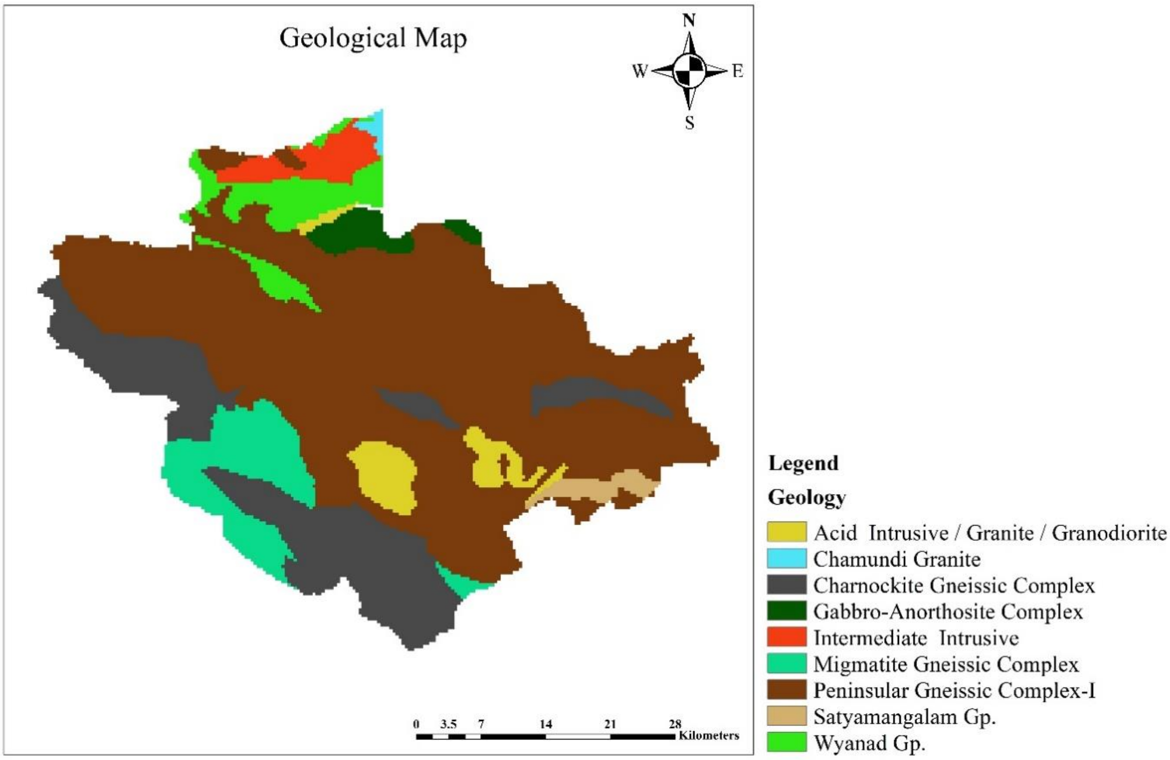

Fig. 6: Geological distributions over the Wayanad landslide district

Dolerite and gabbro intrusions occur in older formations and large lenticular bodies of gabbro/anorthosite exist northeast of Mananthavady, while a substantial diorite body is present near the district's northern boundary[46]. The spatial distribution of geological map is shown in figure 6.

Geomorphological map of the Wayanad: Wayanad district features mainly grouped into two physiographic zones as shown in figure 7. The western hilly terrain aligned with the Western Ghats and the eastern Wayanad plateau. Elevations range from 700 to 2061 meters above sea level, with the district's highest peak, Banasura Hill, situated in Vythiri taluk[28]. The Wayanad plateau slopes are eastward, bordered by structural-denudational hills to the west and isolated structural hills to the east. Unique to Wayanad, the major river systems including the Kabani River, flow eastward. Kabani's tributaries include Mananthavady Puzha, Karumanthodu and Panamarampuzha, while Valapattanam, Kuttiyadi and Chaliyar Rivers drain the western part[50]. Topographically, Wayanad is divided into multiple zones such as rugged high ranges, moderately rugged high ranges, inter-montane valleys and floodplains.

The high ranges in the west, northwest and southwest, with elevations from 1400 to 2100 meters, feature dense mixed forests and rugged terrain with steep slopes. Eastern hill ranges and isolated hills have moderate slopes with elevations between 1000 and 1400 meters. Inter-montane valleys, formed by erosional and depositional processes, occupy areas between high ranges[27].

The floodplains, with alluvial deposits over 10 meters thick, serve as productive aquifers. Landforms in Wayanad include alluvial plains, floodplains, valley fills, linear ridges, hill crests, sloping terrain, rocky slopes and hilly terrain. The floodplain and valley fills are major fluvial landforms while moderately sloping, highly sloping terrains, rocky slopes, linear ridges and hill crests constitute significant denudational landforms[30]. Steep slopes, like the scarp face with a 90° inclination, present challenging terrain, though areas with gentler slopes support promising groundwater zones, contrasting with the unproductive nature of denudational landforms[29].

Lithological distributions: The district exhibits four major soil types of laterite soil, brown hydromorphic soil, forest loam and riverine alluvium. Laterite soil, prevalent in parts of Wayanad, is reddish-brown, formed under a tropical monsoonal climate with alternating wet and dry seasons[31]. This soil contains low organic matter but moderate levels of nitrogen, phosphorus and potash, with a pH range of 5.5 - 6.5 and a clayey loam to silty loam texture. Laterites on high ground are more compact compared to those in low-lying areas[32].

Forest soil, common in the blocks of Mananthavady, Kalpetta and Sultan Bathery, is rich in organic matter, nitrogen and humus, with a slightly acidic pH of 5.3 - 6.3 and a dark reddish-brown loamy texture. The spatial distribution of soils over the Wayanad region is shown in figure 8. Brown hydromorphic soil (BHS), found between undulating landscapes, is deep brown with sandy loam to clayey texture, formed through transported and deposited materials from hill slopes. BHS has a pH of 5.2 - 6.3 and is slightly acidic[33].

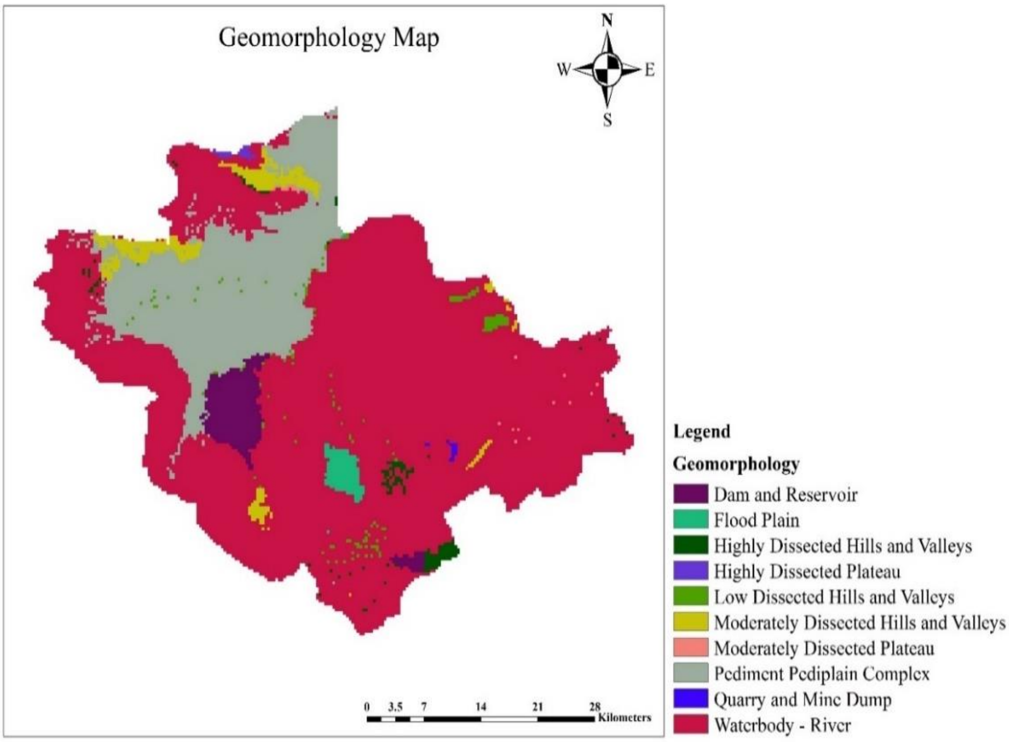

Fig. 7: Geomorphological distributions over the Wayanad landslide district

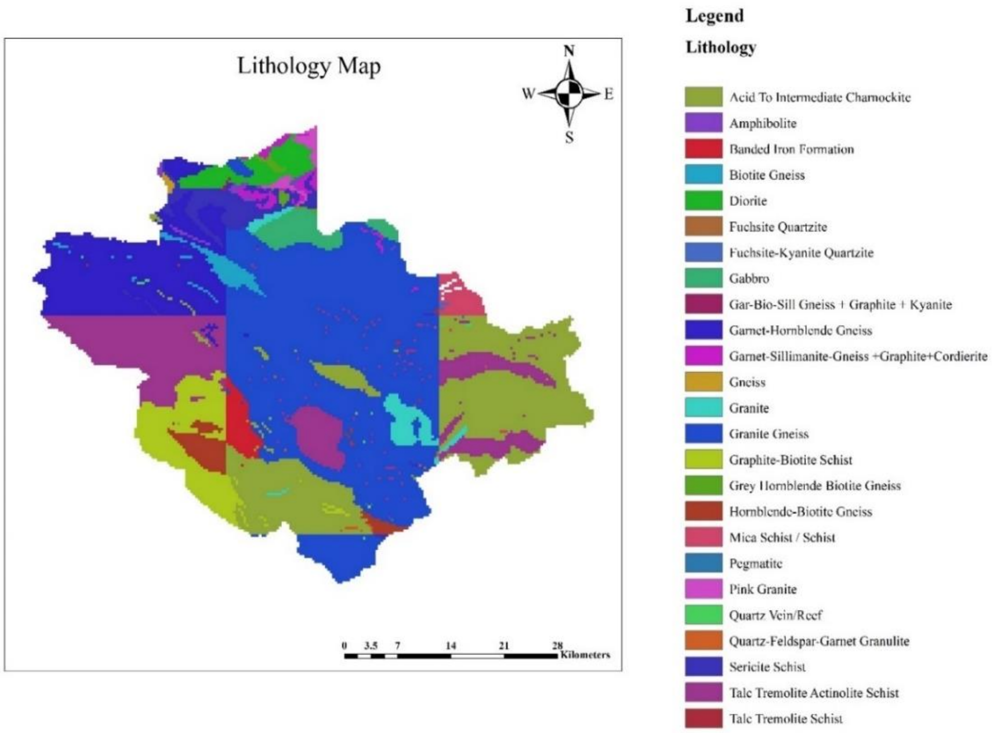

Fig. 8: Lithological distributions over the Wayanad landslide district

Riverine alluvium is present along the banks of the Kabani, Chaliyar and their tributaries. This soil is deep, with a sandy loam to clayey loam texture and historically supported paddy cultivation, now largely replaced by crops such as plantains[34]. Riverine alluvium also contains moderate levels of organic matter, nitrogen, phosphorus and potash.

Land Use Land Cover (LULC) and Landslide Inventory mapping: Wayanad's landscape is predominantly covered by plantation crops such as coffee, tea, rubber, cocoa and pepper, which serve as the district's primary cash crops[36]. The fertile soil also supports the cultivation of spices like cardamom, turmeric and ginger. However, the natural forest areas are increasingly diminishing due to encroachment and conversion into plantation lands[35]. This region, part of the tropical forest biome, is rich in biodiversity and home to several rare plant species. Arable land is scarce and primarily found in narrow valleys, used for cultivating paddy, horticulture, coconut and arecanut. The LULC map (Figure 9) classifies the land into various categories including deciduous broadleaf forest, cropland, built-up land, mixed forest, shrubland, barren land, fallow land, water bodies, plantations, grassland and evergreen broadleaf forest, providing critical insights into land cover changes and their role in landslide susceptibility[39].

The landslide inventory map (Figure 9), documenting 680 landslides, reveals a significant correlation between landslides and proximity to faults, rivers and lineaments, with many landslides occurring near the Bhavali Fault. Additionally, proximity analysis of schools, hospitals and public gathering areas to faults and lineaments is shown in figure 10, highlighting potential risks to critical infrastructure[38]. The flow direction and accumulation maps (Figure 11), with flow direction values ranging from 1 to 128 and accumulation categorized into three major classes (0-5000, 5100-490000 and 500000-1400000), offer essential insights into water movement and areas prone to water-induced landslides. These thematic maps, integrated using GIS and analysed through the AHP technique, are crucial for developing a comprehensive and reliable landslide susceptibility map for Wayanad[37].

Features with re-classified maps: In the Wayanad landslide susceptibility study, several re-classified factors were analysed to create the Landslide Susceptibility Maps (LSMs). The lithological map is crucial because different rock types have varying levels of vulnerability to landslides[51]. Using data sourced from Bhukosh, this map was developed to categorize rock units into susceptibility levels low, moderate and high each assigned a score from 1 to 5, indicating increasing sensitivity to landslides. Elevation and land use are also vital in assessing landslide risk. The land use map includes categories such as irrigated and dry farming, moderate rangeland, sparse forests and barren land, each contributing differently to landslide susceptibility.

The elevation map considers the relationship between altitude and environmental factors like rainfall and frost, with higher altitudes often showing greater vulnerability. Altitude classes of 2230 meters and 126 meters were specifically analysed, with their respective susceptibilities evaluated using the AHP[40].

MCDM techniques: The AHP method was applied for weighing these factors, involving expert evaluations through structured comparison matrices. The consistency of their judgments was checked using the consistency ratio (CR), derived from the consistency index (CI) and the random consistency index (RI)[41]. A CR value of 0.1 or lower indicated acceptable consistency, confirming that no further adjustments were necessary. This rigorous process ensured the reliability of the weighted factors in constructing an accurate landslide susceptibility model for Wayanad[43]. The functional forms of the CR and CI are represented as equation 1 and 2 and the RI values are mentioned in table 1[41]. The accuracy assessment of the LULC Kappa coefficient (k) is summarized in table 2.

Several factors such as elevation, aspect, slope, distance from road, river, faults, lineaments, LULC, TWI, rainfall, lithology, geology and geomorphology have been considered and the comparison matrix for the classes of each factor, with CR values less than 1.10, are summarized in table 3[51,53]. The equation 3 has been used to integrate the weights that's obtained and to generate the LSM of the Wayanad[42].

$$CR = \frac{CI}{RI} \tag{1}$$

$$CI = \frac{\lambda_{max} - n}{n-1} \tag{2}$$

$$LSM_{AHP} = \sum_{j=1}^{n} \sum_{i=1}^{m} \left(w_{ij,AHP} \times w_{j,AHP} \right) \tag{3}$$

The Aspect and Topographic Wetness Index (TWI) play crucial roles in understanding the terrain's influence on landslide occurrences. Utilizing AHP and frequency ratio FR models, these factors are integrated to develop a comprehensive LSM[52]. The aspect, which refers to the direction of the slope, significantly impacts moisture retention, solar radiation and wind exposure, all of which influence the stability of the terrain[46].

The spatial distribution map of aspect, presented in figure 12, categorizes the landscape into different directional classes: Flat (-1), North (0-22.5°), Northeast (22.5-67.5°), East (67.5-112.5°), Southeast (112.5-157.5°), South (157.5-202.5°), Southwest (202.5-247.5°), West (247.5-292.5°) and Northwest (292.5-337.5°). Each aspect class affects the probability of landslide occurrence differently, with certain orientations being more prone to instability due to factors like solar exposure and prevailing winds[47].

Table 1
RI values for different unit[39,40]

n	1	2	3	4	5	6	7	8	9	10
RI	0	0	0.52	0.89	1.11	1.25	1.35	1.4	1.45	1.49

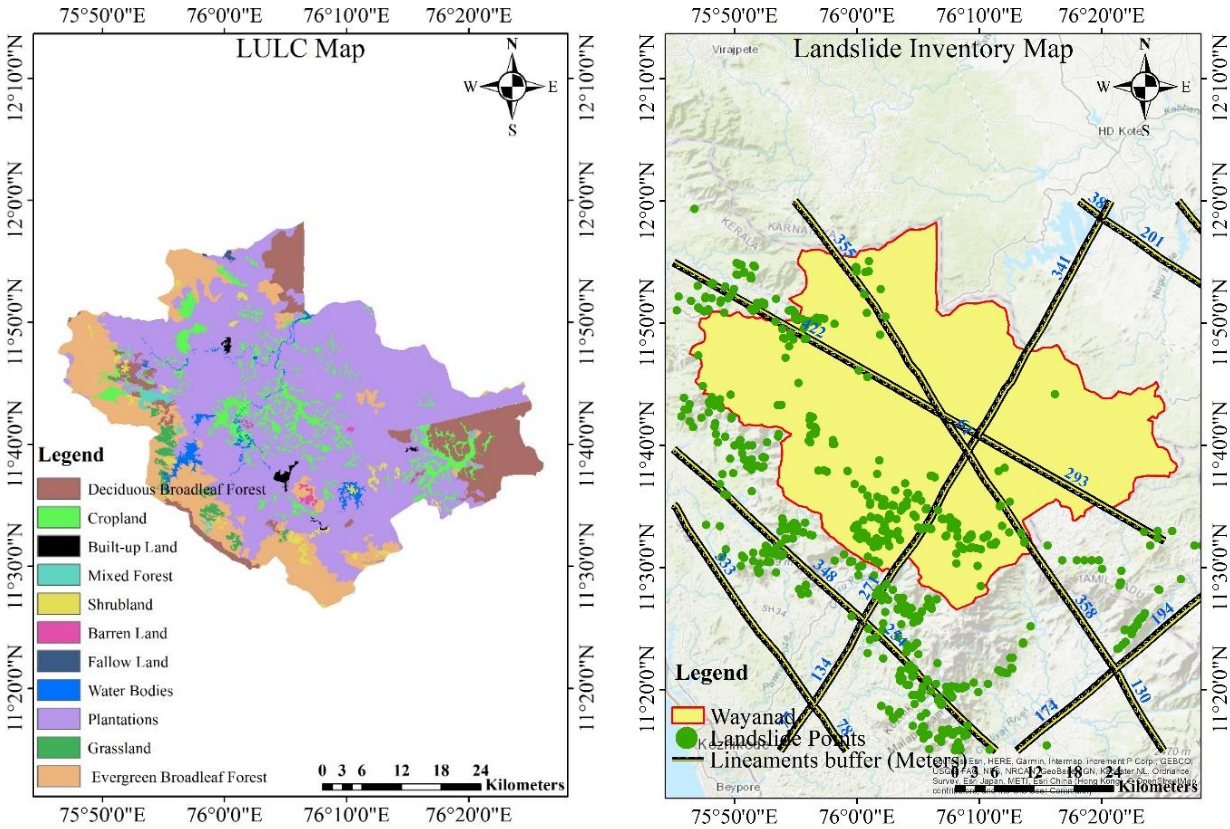

Fig. 9: LULC and landslide inventory maps showing the various lands classes and spatial distribution of historical landslides including lineaments orientation.

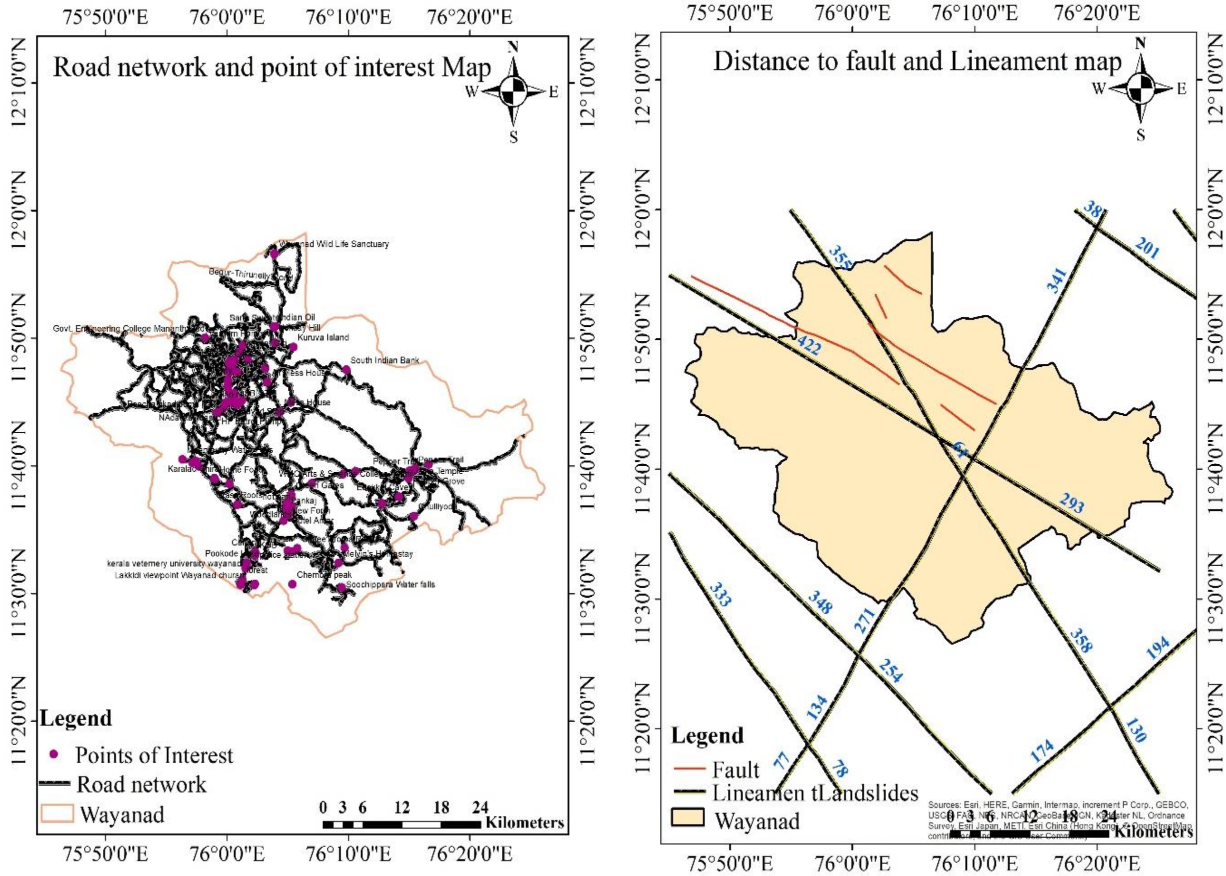

Fig. 10: Internal road network with points of interests, faults and lineaments details over the Wayanad district.

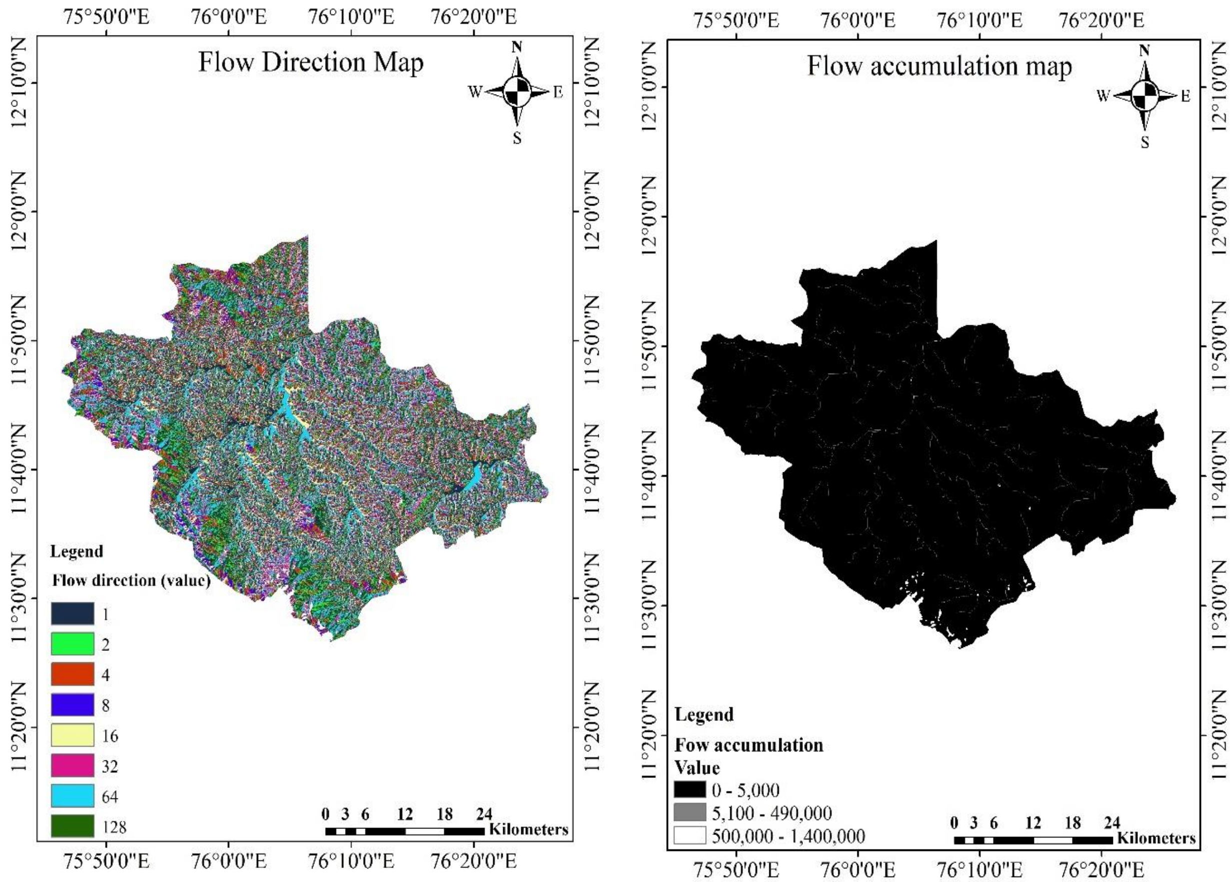

Fig. 11: Flow direction and accumulation over the Wayanad district

Table 2
The accuracy assessment of the LULC Kappa Coefficient (k)

LULC major class		**Water**	**Vegetation**		**Agri. land**	**Built-up land**	**Bare land**	**Total (user)**
			Dense	**Light**				
		1	2	3	4	7	8	50
Water body	1	49	0	0	1	0	0	50
Vegetation (Dense)	2	0	42	4	2	0	2	50
Vegetation (Light)	3	0	2	33	8	1	6	50
Agri.land	4	2	0	6	39	2	1	50
Built-up area	7	0	1	3	6	40	0	50
Bare land	8	3	0	2	0	0	45	50
Sum of producer		54	45	48	56	43	54	300
Overall accuracy								**85.30%**
K-coefficient								**0.82**

The TWI, illustrated in figure 13, measures the potential for water accumulation in the landscape, influencing soil moisture content and consequently, landslide susceptibility. The TWI classes range from -17 to -8.6, -8.5 to -6.7, -6.6 to -4.5, -4.4 to -1.2 and -1.1 to 12. Higher TWI values typically indicate areas with greater moisture accumulation, which can lead to increased soil saturation and a higher likelihood of landslides. Conversely, lower TWI values suggest drier conditions with reduced landslide risk[45].

Frequency Ratio (FR) Method: This method leverages historical data to predict the likelihood of future events and is commonly applied in various studies. It establishes the spatial relationship between landslide occurrences and each conditioning factor[39,48]. The FR indicates the probability of landslide occurrence, with higher FR values signifying a greater likelihood of landslides and a corresponding increase in hazard level. The FR for each class of all conditioning factors is calculated using equation 4:

$$FR_i = \frac{\left({LS_i}/{LS}\right)}{\left(\frac{A_i}{A}\right)} \tag{4}$$

This method leverages historical data to predict the likelihood of future events and is commonly applied in various studies. It establishes the spatial relationship between landslide occurrences and each conditioning factor. The FR indicates the probability of landslide occurrence, with higher FR values signifying a greater likelihood of landslides and a corresponding increase in hazard level[49]. The FR for each class of all conditioning factors is calculated using equation 4. In this context, FR_i is the frequency ratio of the i^{th} class, LS_i represents the total landslide area (number of landslide pixels) in the i^{th} class, LS is the total landslide area (total number of landslide pixels) in the study area, A_i denotes the area under the i^{th} class (total number of pixels in the i^{th} class) and A is the total area.

$$RF_i\left(\frac{FR_i}{\sum FR}\right) \tag{5}$$

$$R_j = MAX\left(RF_{i,j}\right) - MIN\left(RF_{i,j}\right) \tag{6}$$

$$PR_j = {R_j}/{MIN\ (R)} \tag{7}$$

The FR values for different classes (as shown in table 4) are then utilized to determine the Prediction Rate (PR) of each factor, reflecting the weight of each individual factor. This is achieved using equations 5-7, where RF is the relative frequency, $MAX\left(RF_{i,j}\right)$ is the maximum RF value of the j^{th} factor, $MIN\left(RF_{i,j}\right)$ is the minimum RF value of the j^{th} factor and PR_j is the prediction rate of the j^{th} factor. The prediction rate PR_j serves as the weight $W_{j,FR}$ for the j^{th} factor.

Finally, to create the landslide susceptibility map, the FR values for different classes of influencing parameters and the $W_{j,FR}$ for each parameter are combined and summed, as outlined using equation 8:

$$LSM_{FR} = \sum_{j=1}^{n}\sum_{i=1}^{m}\left(FR_{ij} \times W_{j,FR}\right) \tag{8}$$

Validation of the models: In landslide susceptibility studies, validating the model is an essential step to determine its prediction accuracy. For this purpose, the created LSMs are compared with a testing dataset, which includes 30% of the landslide inventory locations[50]. The model's performance is evaluated using the Receiver Operating Characteristic (ROC) curve, which plots the true positive rate (sensitivity) against the false positive rate (specificity). The area under the curve (AUC) serves as a critical metric for measuring prediction accuracy, as highlighted by several researchers[53]. Higher AUC values signify better model performance, with values ranging from 0.5 to 1. Shahabi and Hashim[44] suggest that an AUC value exceeding 0.8 indicates a well-fitting model, a finding supported by Yilmaz[53]. Figure 14 presents the ROC curves for AHP and FR models used in this study.

Accuracy of landslide susceptibility map: The LSM generated using the AHP and FR approaches was validated through ROC curves and AUC methodology shown in figure 14. A total of 680 landslide testing datasets were employed for this validation process[3]. While the ROC curve can also be constructed using the training dataset known as the success rate curve, this method is not considered an accurate approach for assessing the predictive capability of the models. Therefore, the present study adopts the ROC curve derived exclusively from the testing dataset[23].

The ROC curve created using the testing dataset, referred to as the prediction curve for two models, is depicted in figure 14. A comparison of the AUC values indicates that the AHP and FR model delivered the highest prediction accuracy, with an AUC of 0.913 and 0.896. It is noteworthy that all models demonstrate good predictive accuracy, as evidenced by AUC values exceeding 0.8 in both the approaches. The LSMs developed using both AHP and FR approach are shown in figures 15. The LSMs maps are divided into 5 classes such as very low, low, moderate, high and very high susceptibility[14,17].

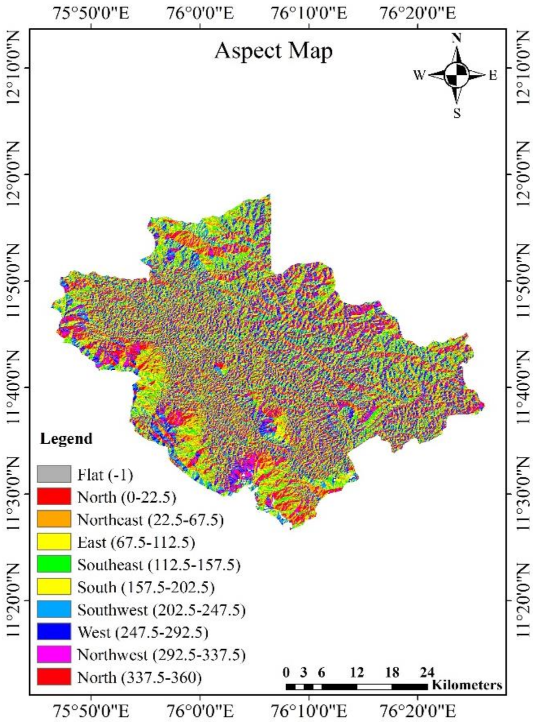

Fig. 12: Aspect map representing the direction that a slope faces on a terrain over the Wayanad district.

Table 3
Pairwise matrix constructed for comparison of matrix and weights that assigned to each of the factor using AHP approach

S.N.	Conditioning	1	2	3	4	5	6	7	8	9	10	11	12	Criteria Weight ($W_{j,AHP}$)
1	Elevation			1	2	3	5	3	2	1	2	0.50	0.33	0.070
2	Slope	1	3	3	4	1	5	4	3	2	2	2	3	0.150
3	Aspect		1	2	3	0.33	1	1.00	1.00	0.50	0.50	0.33	1.00	0.046
4	TWI							1	1.00	1	0.50	0.33	0.33	0.049
5	LULC								1	3	2	1.00	0.50	0.079
6	NDVI									1	2	1	0.50	0.071
7	Rainfall												1	0.133
8	Geomorphology										1	0.50	0.33	0.060
9	Geology											1	0.50	0.091
10	Lithology											1	0.50	0.089
11	Distance from river				1	0.33	1	0.50	0.33	0.33	0.50	0.33	0.20	0.024
12	Distance from road					1	2	3	1	2	3	2.00	0.50	0.092
13	Distance from fault						1	0.50	0.25	0.20	0.33	0.25	0.14	0.020
CR														**0.048**

Table 4
Landslide Pixels (%) classes of each thematic map with assigned weights using FR model

Factor	**Class**	**Pixels (%)**	**Landslide Pixels (%)**	**FR**	**PR (W_j, FR)**
Elevation (m)	<126	28.73	28.05	0.92	1.01
	200-400	14.60	12.58	0.84	
	400-600	11.75	10.87	1.12	
	600-800	12.46	9.57	0.83	
	800-100	11.12	8.98	0.88	
	1000-1500	8.07	12.35	1.54	
	1500-2000	6.89	11.34	1.79	
	>2000	8.90	5.47	0.64	
Slope (degrees)	<15°	47.80	4.35	0.07	4.87
	15°-25°	35.11	17.68	0.53	
	25° - 35°	13.14	29.34	2.41	
	35° - 45°	4.12	33.01	8.14	
	>45°	0.87	15.99	18.65	
Aspect	Flat (-1)	1.86	0.00	0.00	2.01
	North (0-22.5)	6.38	5.07	0.81	
	Northeast (22.5-67.5)	11.59	14.09	1.34	
	East (67.5-112.5)	12.93	14.54	1.14	
	Southeast (112.5-157.5)	13.98	16.54	1.10	
	South (157.5-202.5)	14.89	17.01	1.17	
	Southwest (202.5-247.5)	14.85	15.05	1.15	
	West (247.5-292.5)	12.86	9.01	0.72	
	Northwest (292.5-337.5)	12.87	10.02	0.79	
TWI	- -17 - -8.6	2.17	16.22	8.01	6.01
	-8.5 - -6.7	62.1	69.0	1.15	
	-6.6 - -4.5	24.1	12.00	0.55	
	-4.4 - -1.2	6.8	2.87	0.47	
	-1.1 - 12	5.71	0.91	0.17	
LULC	Waterbodies	0.52	0.45	0.72	5.55
	Dense Vegetation	77.05	78.01	1.07	
	Light Vegetation	18.50	16.57	0.99	
	Agricultural Land	2.91	0.06	0.03	
	Built Area	2.93	2.54	0.74	
	Bare Land	0.05	0.52	8.45	
NDVI	<0.020	0.08	0.02	0.08	2.24
	0.020 - 0.038	1.25	2.68	2.12	
	0.038 - 0.057	2.35	4.17	1.79	
	0.057 - 0.86	12.98	15.24	2.10	
	0.086-0.092	20.14	21.02	1.34	
	0.092-0.999	64.15	57.25	0.99	
Rainfall (mm/year)	<1500	23.15	5.78	0.27	4.24
	1500 - 2000	47.14	28.21	0.59	
	2000-2500	13.17	17.21	1.24	
	2500-3000	11.67	25.14	2.15	
	>3000	4.78	25.89	5.43	
Geomorphology	Alluvial Plain	14.56	39.12	2.87	3.17
	AT	31.04	3.17	0.17	
	HDHV	41.50	14.85	0.34	
	LDP	0.27	0	0.00	
	MDHV	0.98	0.03	0.03	
	PPC	2.54	4.68	1.87	
	MDH	11.39	39.65	3.47	
Lithology	Fs	3.17	0.01	0.00	5.54

	BHS	6.18	2.89	0.44	
	RA	23.99	35.01	0.42	
	MS	2.98	23.00	7.83	
	LP	12.41	8.01	0.66	
	PPS	50.99	33.10	0.67	
Distance from river (m)	<200	8.35	4.12	0.51	1.17
	200 - 400	8.01	6.67	0.93	
	400 - 600	7.45	6.14	0.91	
	600 - 800	7.04	6.28	0.87	
	>800	69.47	77.21	1.12	
Distance from road (m)	<200	5.87	22.14	3.62	2.56
	200 - 400	5.14	7.58	1.42	
	400 - 600	4.65	10.89	2.38	
	600 - 800	4.25	6.24	1.45	
	>800	80.14	54.12	0.68	
Distance from faults (m)	<500	7.14	5.21	0.71	1.58
	500 - 1500	7.08	7.00	1.12	
	1500 - 3000	6.99	13.65	1.90	
	3000 - 3500	6.89	13.14	1.96	
	>4500	72.01	62.38	0.92	

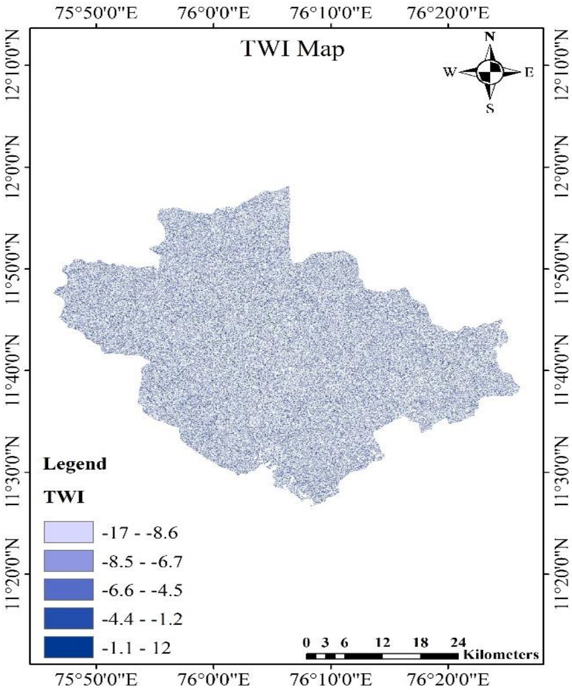

Fig. 13: Topographic wetness index map of Wayanad showing the potential water accumulation

Conclusion

The study effectively demonstrates the integration of GIS, AHP and FR models in creating a reliable landslide susceptibility map for Wayanad district. Key conclusions include:

- The multi-step methodology, involving data collection, thematic map creation and MCDM application, ensures comprehensive analysis of landslide susceptibility factors.
- AHP and FR models provide robust frameworks for weight determination with CR and AUC values confirming the reliability and predictive accuracy of the LSM.
- The LSM categorizes Wayanad into five susceptibility classes, highlighting areas at varying risks of landslides, which is crucial for targeted risk mitigation and disaster management.
- Validation results, with AUC scores above 0.8, confirm the models' high predictive performance, underscoring the efficacy of the applied methodologies.
- The study emphasizes the critical need for systematic landslide susceptibility mapping and the role of sustainable land use practices in mitigating landslide risks in Wayanad.

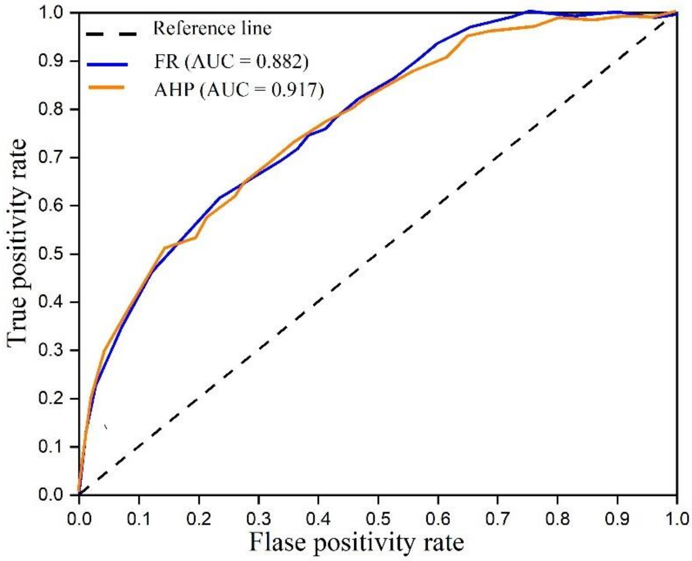

Fig. 14: ROC curves corresponding to testing data set using AHP and FR models

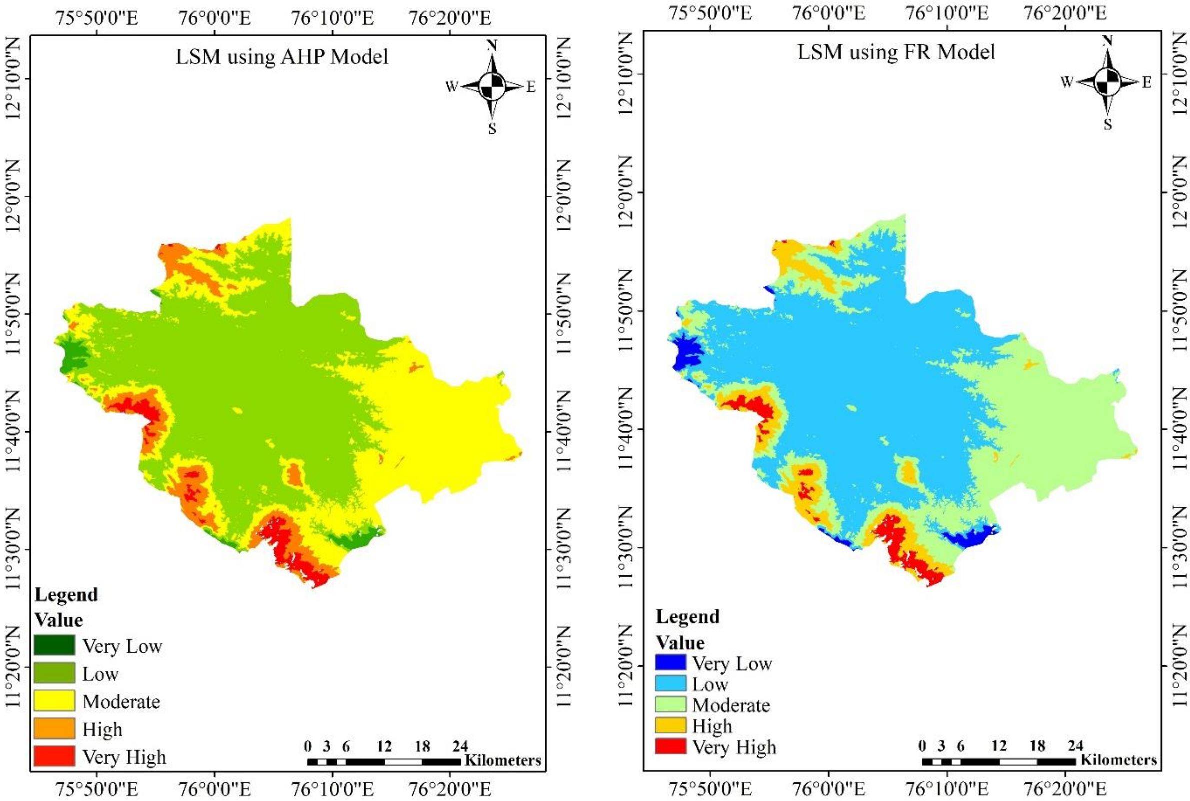

Fig. 15: Landslide susceptibility map of Wayanad using AHP and FR models

References

1. Abedini M. and Tulabi S., Assessing LNRF, FR and AHP models in landslide susceptibility mapping index: a comparative study of Nojian watershed in Lorestan province, Iran, *Environmental Earth Sciences*, **77(11)**, 405-412 **(2018)**

2. Abella E.A.C. and Van Westen C.J., Qualitative landslide susceptibility assessment by multicriteria analysis: a case study from San Antonio del Sur, Guantánamo Cuba, *Geomorphology*, **94(3-4)**, 453-466 **(2008)**

3. Acharyya Nirupam, Bandyopadhyay Jatisankar and Das Suman, Assessment of cyclone induced flood using microwave Synthetic Aperture Radar (SAR) data in four blocks of East Midnapore district, India, *Disaster Advances*, **17(4)**, 40-47 **(2024)**

4. Achu A. and Reghunath R., Application of analytical hierarchy process (AHP) for Landslide Susceptibility Mapping: A study from southern Western Ghats, Kerala, India, Disaster, Risk and Vulnerability Conference 2017, 33-39 **(2017)**

5. Aditian A., Kubota T. and Shinohara Y., Comparison of GIS-based landslide susceptibility models using frequency ratio, logistic regression and artificial neural network in a tertiary region of Ambon, Indonesia, *Geomorphology*, **318**, 101-111 **(2018)**

6. Althuwaynee O.F., Pradhan B. and Lee S., A novel integrated model for assessing landslide susceptibility mapping using CHAID and AHP pair-wise comparison, *International Journal of Remote Sensing*, **37(5)**, 1190-1209 **(2016)**

7. Asmare D., Application and validation of AHP and FR methods for landslide susceptibility mapping around Choke Mountain, northwestern Ethiopia, *Scientific African*, **19**, e01470 **(2023)**

8. Babitha B.G., Danumah J.H., Pradeep G.S., Costache R., Patel N., Prasad M.K., Rajaneesh A., Mammen P.C., Ajin R.S. and Kuriakose S.L., A framework employing the AHP and FR methods to assess the landslide susceptibility of the Western Ghats region in Kollam district, *Safety in Extreme Environments*, **4(2)**, 171-191 **(2022)**

9. Bhagya S.B., Sumi A.S., Balaji S., Danumah J.H., Costache R., Rajaneesh A., Gokul A., Chandrasenan C.P., Quevedo R.P., Johny A. and Sajinkumar K.S., Landslide susceptibility assessment of a part of the Western Ghats (India) employing the AHP and F-AHP models and comparison with existing susceptibility maps, *Land*, **12(2)**, 468-479 **(2023)**

10. Biswas B., Ks V. and Ranjan R., Landslide susceptibility mapping using integrated approach of multi-criteria and geospatial techniques at Nilgiris district of India, *Arabian Journal of Geosciences*, **14(11)**, 980-991 **(2021)**

11. Biswas B., Rahaman A. and Barman J., Comparative assessment of FR and AHP models for landslide susceptibility mapping for Sikkim, India and preparation of suitable mitigation techniques, *Journal of the Geological Society of India*, **99(6)**, 791-801 **(2023)**

12. Chandra B.R., Akshaya M.P., Sravani B., Ashritha Y.S. and Pavithra B.K., Internet of Things (IoT) based Digital Helmet Design and Deployment, Proceedings of the 2023 7th International Conference on Trends in Electronics and Informatics (ICOEI), 397-404 **(2023)**

13. Chandra B.R. and Kumar K., A Comprehensive Study on a Meta Heuristics Optimization Algorithm- Hybridized Mayfly Algorithm, Proceedings of the 2022 6th International Conference on Trends in Electronics and Informatics (ICOEI), 1649-1655 **(2022)**

14. Chandra B.R., Pranitha C., Preethi A.E., Pavani K., Rajini M. and Bai H.M., Implementation of Ripple Carry Adder Using Full Swing Gate Diffusion Input, Proceedings of the 2023 7th International Conference on Trends in Electronics and Informatics (ICOEI), 44-50 **(2023)**

15. Chanu M.L. and Bakimchandra O., Landslide susceptibility assessment using AHP model and multi resolution DEMs along a highway in Manipur, India, *Environmental Earth Sciences*, **81(5)**, 156-163 **(2022)**

16. Chimidi G., Raghuvanshi T.K. and Suryabhagavan K.V., Landslide hazard evaluation and zonation in and around Gimbi town, western Ethiopia-a GIS-based statistical approach, *Applied Geomatics*, **9(4)**, 219-236 **(2017)**

17. Durga M., Shoba K.B., Thangavelu R., Ravikanth S., Sasikala R., Rajasekaran B. and Ramachandran G., Analysis of IoT and Artificial Intelligence Smart Transportation System Application Technology, Proceedings of the 2024 International Conference on Advances in Modern Age Technologies for Health and Engineering Science (AMATHE), 1-7 **(2024)**

18. Eitvandi N., Sarikhani R. and Derikvand S., Landslide susceptibility mapping by integrating analytical hierarchy process, frequency ratio and fuzzy gamma operator models, case study: North of Lorestan Province, Iran, *Environmental Monitoring and Assessment*, **194(9)**, 600 **(2022)**

19. Gupta N., Pal S.K. and Das J., GIS-based evolution and comparisons of landslide susceptibility mapping of the East Sikkim Himalaya, *Annals of GIS*, **28(3)**, 359-384 **(2022)**

20. Hung L.Q., Van N.T.H., Duc D.M., Ha L.T.C., Van Son P., Khanh N.H. and Binh L.T., Landslide susceptibility mapping by combining the analytical hierarchy process and weighted linear combination methods: a case study in the upper Lo River catchment (Vietnam), *Landslides*, **13(5)**, 1285-1301 **(2016)**

21. Kumar R. and Anbalagan R., Landslide susceptibility mapping using analytical hierarchy process (AHP) in Tehri reservoir rim region, Uttarakhand, *Journal of the Geological Society of India*, **87**, 271-286 **(2016)**

22. Kumar Madan, Kumar Vijay, Kumar Kunal, Kumar Ashish and Priyadarshee Akash, Seismic effect of steel bracing systems in RC frame models, *Disaster Advances*, **17(1)**, 35-43 **(2024)**

23. Lalrindika PC., Zonunsanga R. and Rinawma P., Integrated Analytical Hierarchy Process (AHP) and GIS techniques based Soil Erosion Susceptibility Mapping in Chite Watershed, Mizoram, India, *Disaster Advances*, **17(3)**, 25-34 **(2024)**

24. Lavuri N., Immadi G. and Narayana M.V., Design of Tri-Band Hybrid Dielectric Resonator Antenna for Wireless Applications. *Progress In Electromagnetics Research Letters*, **98**, 75-84 **(2021)**

25. Lavuri N., Immadi G. and Narayana M.V., Design of Tri-Band Hybrid Dielectric Resonator Antenna for Wireless Applications, *Progress In Electromagnetics Research Letters*, **98**, 75-84 **(2021)**

26. Lavuri N., Immadi G., Narayana M.V., Ambati N., Aovuthu S.M. and Kolasani R., A Compact Multiband Hybrid Rectangular DRA for Wireless Applications, *Progress In Electromagnetics Research Letters*, **117**, 89-96 **(2024)**

27. Malik Arshid Hussain and Uma Devi Randhi, An advanced GIS based approach for the assessment of coastal inundation in the storm surge region (Krishna District) of Andhra Pradesh, INDIA, *Disaster Advances*, **17(5)**, 34-49 **(2024)**

28. Majumder S. and Fatma R., Assessing Landslide Susceptibility Mapping in Shimla District, Himachal Pradesh, India: A Comparative Approach Using Fuzzy-AHP and FR for Risk Prediction, Landslides in the Himalayan Region: Risk Assessment and Mitigation Strategy for Sustainable Management, 301-333 **(2024)**

29. Mandal B. and Mandal S., Analytical hierarchy process (AHP) based landslide susceptibility mapping of Lish river basin of eastern Darjeeling Himalaya, India, *Advances in Space Research*, **62(11)**, 3114-3132 **(2018)**

30. Mandal S., Maiti R., Mandal S. and Maiti R., Application of analytical hierarchy process (AHP) and frequency ratio (FR) model in assessing landslide susceptibility and risk, Semi-Quantitative Approaches for Landslide Assessment and Prediction, 191-226 **(2015)**

31. Mondal S. and Maiti R., Integrating the analytical hierarchy process (AHP) and the frequency ratio (FR) model in landslide susceptibility mapping of Shiv-khola watershed, Darjeeling Himalaya, *International Journal of Disaster Risk Science*, **4**, 200-212 **(2013)**

32. Myronidis D., Papageorgiou C. and Theophanous S., Landslide susceptibility mapping based on landslide history and analytic hierarchy process (AHP), *Natural Hazards*, **81**, 245-263 **(2016)**

33. Nageswara Rao L., Immadi G. and Narayana M.V., A compact hybrid dielectric resonator antenna for multiband in wireless applications, *International Journal of Speech Technology*, **24**, 737-746 **(2021)**

34. Pham B.T., Prakash I., Khosravi K., Chapi K., Trinh P.T., Ngo T.Q., Hosseini S.V. and Bui D.T., A comparison of Support Vector Machines and Bayesian algorithms for landslide susceptibility modelling, *Geocarto International*, **34(13)**, 1385-1407 **(2019)**

35. Potekar U.P., Naik D.D. and Patil A.S., Geospatial approach for Landslide Susceptibility Mapping techniques: A Case Study of Ratnagiri District, Maharashtra, India, *Disaster Advances*, **16(4)**, 34-45 **(2023)**

36. Rao L.N. and Ramesh B., A compact hybrid cylindrical dielectric resonator antenna for WLAN applications, 2017 International Conference on Energy, Communication, Data Analytics and Soft Computing (ICECDS), Chennai, India, 3390-3393 **(2017)**

37. Rao L.N., Design of dual-band dielectric resonator antenna with slot for WLAN applications, 2017 IEEE International Conference on Power, Control, Signals and Instrumentation Engineering (ICPCSI), Chennai, India, 2371-2374 **(2017)**

38. Roy J. and Saha S., Landslide susceptibility mapping using knowledge-driven statistical models in Darjeeling District, West Bengal, India, *Geoenvironmental Disasters*, **6(1)**, 1-18 **(2019)**

39. Saaty T.L., Decision making with the analytic hierarchy process, *International Journal of Services Sciences*, **1(1)**, 83-98 **(2008)**

40. Saaty T.L., Fundamentals of decision making and priority theory with the analytic hierarchy process, Analytic Hierarchy Process Series, RWS Publications, Pittsburgh **(2000)**

41. Sabatakakis N., Koukis G., Vassiliades E. and Lainas S., Landslide susceptibility zonation in Greece, *Natural Hazards*, **65(1)**, 523-543 **(2013)**

42. Salehpour Jam A., Mosaffaie J., Sarfaraz F., Shadfar S. and Akhtari R., GIS-based landslide susceptibility mapping using hybrid MCDM models, *Natural Hazards*, **108**, 1025-1046 **(2021)**

43. Sangchini E.K., Emami S.N., Tahmasebipour N., Pourghasemi H.R., Naghibi S.A., Arami S.A. and Pradhan B., Assessment and comparison of combined bivariate and AHP models with logistic regression for landslide susceptibility mapping in the Chaharmahal-e-Bakhtiari Province, Iran, *Arabian Journal of Geosciences*, **9**, 1-15 **(2016)**

44. Shahabi H. and Hashim M., Landslide susceptibility mapping using GIS-based statistical models and remote sensing data in tropical environment, *Scientific Reports*, **5(1)**, 1-15 **(2015)**

45. Sharma S. and Mahajan A.K., A comparative assessment of information value, frequency ratio and analytical hierarchy process models for landslide susceptibility mapping of a Himalayan watershed, India, *Bulletin of Engineering Geology and the Environment*, **78**, 2431-2448 **(2019)**

46. Souissi D. et al, GIS-based MCDM–AHP modeling for food susceptibility mapping of arid areas, southeastern Tunisia, *Geocarto International*, **35(9)**, 991-1017 **(2020)**

47. Tesfa C., GIS-Based AHP and FR Methods for Landslide Susceptibility Mapping in the Abay Gorge, Dejen–Renaissance Bridge, Central Ethiopia, *Geotechnical and Geological Engineering*, **40(10)**, 5029-5043 **(2022)**

48. Thomas A.V., Saha S., Danumah J.H., Raveendran S., Prasad M.K., Ajin R.S. and Kuriakose S.L., Landslide susceptibility zonation of Idukki district using GIS in the aftermath of 2018 Kerala floods and landslides: a comparison of AHP and frequency ratio methods, *Journal of Geovisualization and Spatial Analysis*, **5**, 1-27 **(2021)**

49. Upadhyaya A.N., Muthukumar K., Paul N.R. and Ravikanth S., Advancing Safety: IoT-Based Multi Sensor System for Real-Time Multiple Hazards Detection and Alarming, 2023 4th International Conference on Smart Electronics and Communication (ICOSEC), 404-410 **(2023)**

50. Veerappan R., Negi A. and Siddan A., Landslide susceptibility mapping and comparison using frequency ratio and analytical hierarchy process in part of NH-58, Uttarakhand, India, Advancing Culture of Living with Landslides: Volume 2 Advances in Landslide Science, 1081-1091 **(2017)**

51. Wang Q. and Li W., A GIS-based comparative evaluation of analytical hierarchy process and frequency ratio models for landslide susceptibility mapping, *Physical Geography*, **38(4)**, 318-337 **(2017)**

52. Yan F., Zhang Q., Ye S. and Ren B., A novel hybrid approach for landslide susceptibility mapping integrating analytical hierarchy process and normalized frequency ratio methods with the cloud model, *Geomorphology*, **327**, 170-187 **(2019)**

53. Yilmaz I., Landslide susceptibility mapping using frequency ratio, logistic regression, artificial neural networks and their comparison: a case study from Kat landslides (Tokat-Turkey), *Computers & Geosciences*, **35(6)**, 1125-1136 **(2009)**.

(Received 08th January 2025, accepted 12th February 2025)